Debris Flow event on Osorno volcano, Chile, during summer 2017: New interpretations for chain processes in the Southern Andes.

Ivo Janos Fustos-Toribio[1], Bastian Morales-Vargas[2,3], Marcelo Somos-Valenzuela[3,4*], Pablo Moreno-Yaeger [1,5], Ramiro Muñoz-Ramirez[2], Ines Rodriguez Araneda[2], Ningsheng Chen[6]

[1] Department of Civil Engineering, University of La Frontera, Francisco Salazar 1145, Temuco, Chile

[2] Departamento de Obras Civiles y Geología, Facultad de Ingeniería, Universidad Católica de Temuco, Rudecindo Ortega 02950, Temuco, Chile

[3] Department of Forest Sciences, Faculty of Agriculture and Forest Sciences, Universidad de La Frontera, Av. Francisco Salazar 01145, Temuco, Chile, 4780000

[4] Butamallín Research Center for Global Change, University of La Frontera, Av. Francisco Salazar 01145, Temuco, Chile, 4780000

[5] Department of Geoscience, University of Wisconsin–Madison, 1215 West Dayton St., Madison, WI 53706, USA.

[6] Key Laboratory of Mountain Hazards and Surface Processes, Institute of Mountain Hazards and Environment, Chinese Academy of Sciences, Chengdu 610041, China

Correspondence to: Marcelo Somos (marcelo.somos@ufrontera.cl)

Abstract. Debris flow generation on volcanic zones at the Southern Andes has not widely studied, despite the enormous economic and infrastructure damage that these events can generate. The present work contributes to the understanding of these dynamics based on a study of the 2017 Petrohué debris flow event from two complementary points of view. First, a comprehensive field survey allowed to delimitate that a rockfall initiated the debris-flow due to intense rainfall event. The rockfall lithology corresponds to lava blocks and autobrecciated lavas, predominantly over 1500 m.a.s.l. Second, the process was numerically modeled and constrained by in situ data collection and geomorphological mapping. The event was studied by back analysis using the height of flow measured in road CH-255 with errors of 5%. Debris flow volume has a high sensitivity with the initial water content in the block fall zone, ranging between 4.7×10^5 up to 5.5×10^5 m^3, depending on the digital elevation model (DEM) used. Therefore, debris flow showed that the zone is controlled by the initial water content available previous to the block fall. Moreover, our field data suggest that future debris flows events can take place removing material from the volcanic edifice. We conclude that similar events could occur in the future and that it is necessary to increase the mapping of zones with autobrecciated lava close to the volcano summit. The study contributes to understanding debris flows in the Southern Andes since the Osorno volcano shares similar features with other stratovolcanoes in the region.

1   Introduction

Landslides processes are among the most important natural hazards in developing countries due to their low resilience, generating damage to human life, property, and engineering projects in all the mountainous areas of the world every year

35   (Martha et al., 2010; Alimohammadlou, 2013; Sepúlveda et al., 2014; Fustos et al., 2020). Debris flows are an important type of mass wasting, described as one of the most dangerous of these processes due to their high velocity, the damage that they cause, and the extensive areas affected (Jakob & Hungr, 2005). Nevertheless, debris flows studies in volcanic zones is limited, where only primary volcanic-originated processes like lahars have been studied. The present work evaluates the generation of debris flows, taking the 2017 Petrohué event as a case study. This event caused severe economic losses to one of the most

40   popular tourist attractions in southern Chile (INE, 2018).

Debris flows are very destructive processes in active zone in the Andes, especially in volcanic areas independent of their trigger (Sosio et al., 2011). The northern Andes shows examples like the 1985 Nevados del Ruiz eruption. The volcanic activity triggered a lahar flow, which claimed at least 25,000 lives (Naranjo et al., 1986). In December 1999, a mud and debris flow in Venezuela caused the loss of 30,000 lives (Wieczorek et al., 2000). Rock and soil movements, debris avalanches, debris, and

45   mudflows, and the resulting floods destroyed about 40 km of the Trans-Ecuadorian oil pipeline and the only highway from Quito to Ecuador's northeastern rain forests and oil fields. This phenomenon was caused by heavy rain and two earthquakes in 1987 (Schuster et al., 1996). In 2017, a rainfall-induced landslide event with more than 600 shallow landslides was triggered in Colombia. Following the intense rainfall, landslides and subsequent Mocoa Debris Flow (MDF) event killed to 333 people (García-Delgado et al., 2019). Moreover, the Central Andes has experienced massive debris flow events like the ones in the

50   Lastarria volcano (Rodríguez et al., 2020). The collapse of part of the edifice triggered a 270 km/hr volcanic debris avalanche. Catastrophic debris flows occurred on Huascarán (an extinct volcano), Peru, in 1962 and 1970, triggered by ice and rock, which were swept down from the north peak of the mountain because of an earthquake (Mw 7.9). The 1962 and 1970 events are estimated to have caused ~7,000 deaths (Evans et al., 2009,; Tacconi et al., 2017; Bueechi et al., 2018). Until now, only scarce volcanic related debris flows have been reported in the Southern Andes. An hyperconcentrated flow occurred days after

55   the 2008 volcanic eruption at Chaitén volcano. The trigger of the event is related to intense rainfall over ash deposits within days of cessation of the eruption (Pierson et al., 2013). Therefore, the connection between debris flow and volcanic environments in the Andes has been covered in the past in Northern and Central Andes. However, they are still only superficially studied in the Southern Andes (Korup et al., 2019).

In the Southern Andes, volcanic edifices are covered by materials that could produce recurrent debris flows, molding the relief.

60   The debris flows reported currently in the literature on volcanoes are mainly the result of snow and ice melting during eruptions in lahar form (Johnson and Palma, 2015; Major et al., 2016; Thouret et al., 2020). Nevertheless, few works addresses the relation between the debris flows generated by stratigraphic conditions in volcanic systems and the morphology of the edifice. Their spatial and temporal extension has also been little studied; these are very important since the number of debris flows in volcanic systems has increased in recent years (Pierson, 1995; Aguilar et al., 2014; Korup et al., 2019; Thouret et al., 2020).

65   The present work seeks to advance our comprehension of the generation of debris flows in volcanic edifices in the Southern Andes. An atypical debris flow event of January 8th, 2017 (southern summer) on Osorno volcano (Southern Andes) was assessed. The geomorphological and geological factors influencing the generation of the debris flow event were studied, estimating the conditions which triggered the event through back analysis using the r.avaflow model. Finally, we discuss

whether the event might be recurrent in time or is part of the normal cycle of the volcano; this knowledge will assist in assessing the risk of debris flows in the Southern Andes.

2 Study area

Osorno is a stratovolcano that is part of the active volcanic arc of the southern Andes, called the Southern Volcanic Zone (SVZ). The SVZ is a continuous volcanic arc of 1400 km long, extending from 33.3º to 46i□ S (Stern, 2007; Moreno & Gibbons, 2007). The study area is the south-eastern flank of Osorno volcano (41.1054ºS, 72.4961ºW), beside Route CH-255 (Figure 1), which connects the villages of Ensenada (on the eastern side of the Lake Llanquihue) and Petrohué (on Lake Todos Los Santos).

The area has a total population of 44,578 people with a density of 11.0 per km2. The topography makes CH-255 route the only connection between Petrohué and Ensenada, and regular aero transport is impossible except for a few flights by helicopters, unavailable for the local population. Therefore, CH-255 route becomes a critical infrastructure for local development. This had led to call that route as "El Solitario Pass" (Lonely Pass) Finally, note that the village of Petrohué has a population of 193 people, surpassing 3,000 in summer. The village does not have the capacity for autonomous subsistence, depending on the food and services of Ensenada.

2.1 Geological setting

Osorno volcano is a mainly basaltic Pleistocene to Holocene composite volcano (Figure 1). Its part of an SW-NE volcanic alligment along with three other volcanoes: La Picada, Puntiagudo, and Cordón Cenizos (Moreno et al., 2010), oriented obliquely to the main volcanic arc and the Liquiñe-Ofqui Fault System (LOFS). The chain orientation suggests that the area is an active transtensional zone of the crust, with mafic magma extrusion during the Quaternary (Cembrano & Lara, 2009; Moreno et al., 2010). The surrounding area shows pre-LGM (Last Glacial Maximum) Pleistocene volcanic rocks including tuffs, breccias, and lava originating from the northern zone of the volcano (Moreno et al., 1985).

Alluvial fans in Osorno volcano are composed of unselected sandy rich matrix polymictic gravels, organized in meters thick banks. These form the current filling of the gullies on Osorno volcano, together with alluvial deposits generated by the re-working of moraine deposits and old lahar fans. Debris flows have also been recorded, triggered by snow-melt and intense rainfall in the zone (Moreno et al., 2010). Alluvial deposits exist associated with debris flows and rockfalls in the zone. The granulometry ranges from sand to gravel, and the deposits extend to the shore of the Lake Todos Los Santos (Garrido, 2015).

2.2 Records of rainfall-induced landslides

The zone has suffered recurrent debris flow events during periods of variable precipitation, so the factors which triggered these events are strictly unknown (Garrido et al., 2017; Garrido et al., 2018). For example, debris flows and mudflows occurred on June 2nd, 2015, associated with a front of intense and prolonged precipitation over CH-255 (El Solitario pass). These flows

damaged five houses and four barns, as well as destroying one water tank and some pipework of the second water tank of the drinking water supply network of the village of Petrohué (Garrido, 2015). On January 8th, 2017, large debris flows occurred again on the eastern sector of the volcano's south flank, during a front of intense precipitation. 94 mm of precipitation in a period of 24 hr were recorded in Ensenada, with the 0° isotherm above 3,000 m.a.s.l. The Petrohué debris flow was an atypical event in that it occurred outside the season of intense precipitations; it caused serious material and economic damage to one of the most popular tourist attractions in southern Chile. The road was blocked in 5 different places, and tourists were cut off for several hours in the area of the Saltos de Petrohué (Garrido et al., 2017; Garrido et al., 2018).

Figure 1 Geological map of Osorno volcano based on Moreno et al. (2010).
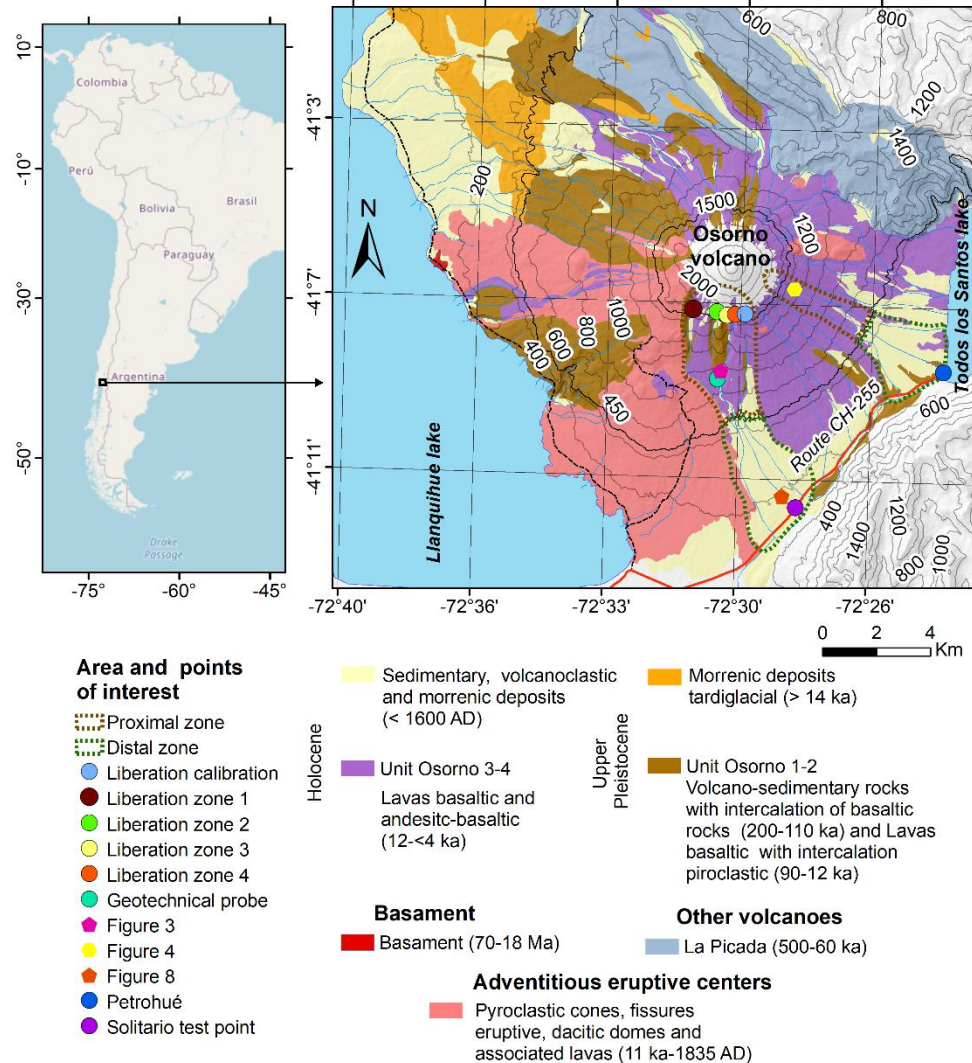
3   Methodology

The 2017 Petrohué event was studied to understand the factors which control the occurrence of debris flows in the Osorno volcano. We implement a methodological approach based on comprehensive numerical modelling constrained by field data and laboratory analysis (Figure 2). We considered geomorphological factors that influenced debris flow generation in field work and defining the release zones. The field results were used as border conditions in numerical modelling of the event by back analysis, taking flow heights recorded in technical reports and photographs to define zones of comparison.

Figure 2 Short methodology.
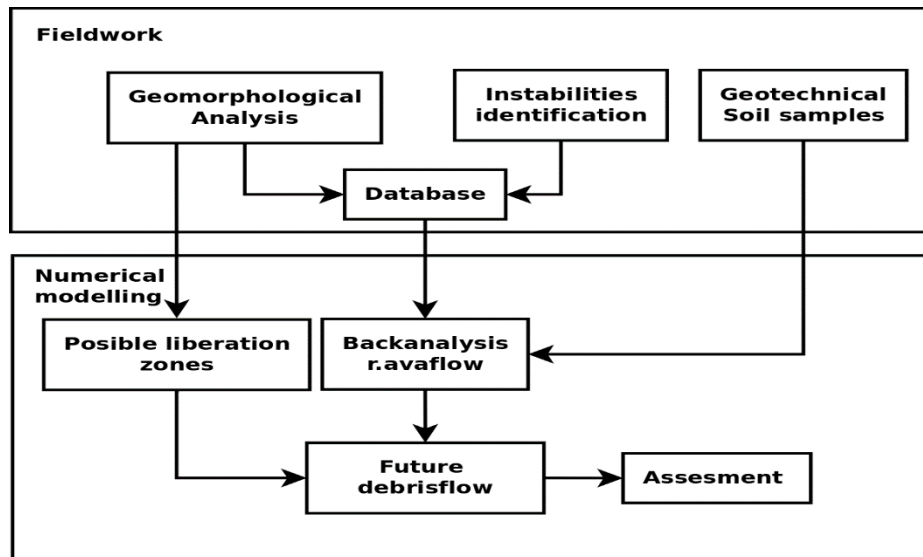
3.1   Field evicence

The mechanisms which generated the 2017 Petrohué debris flow event were studied in the area, approaching by the "El Solitario" pass (41.1943ºS, 72.4759ºW). Areas affected by the flow were identified and mapped in detail. In-situ debris flow deposits analysis is critical to establish a rheological model to be used. Specifically, the grain size distribution transported was assessed, indicating if the flow corresponds to a hyper-concentrated process or not. Hence, geomorphological characteristics were analyzed, noting particularly slopes susceptible to movement in intense precipitation events. The geomorphological features were evaluated by measuring slopes and heights with metric rules and qualitative analysis of depositional structures related to the debris flow.

Due to the extensiveness of the area, elevation and channel gradient data is derived from the two different DEMs, SRTM and ASTER. Additional information regarding distance measurements such as side slopes, channel depth and the maximum width of the landslide was evaluated in the field using metric rulers. Specifically, the width of the landslide is identified and georeferenced using a handle GPS to constrain the numerical modelling results. On the CH-255 road, the final height of debris flows is established as 1.5 m from Garrido et al. (2017). Moreover, debris flow deposits identified in the field allowed

understanding the rheology of these events (non-Newtonian flows). We evaluated debris flow initiation zones close to the
130 Volcano summit and the physical weathering of rock/soil. Scarps with potential rockfalls of unstable blocks were identified, measured, and georeferenced. We established these scarps as initiation debris flow zones (or release zone) in the following numerical model. Finally, debris flow runout was estimated measuring the channel distance between the liberation zone and the CH-255 limit using navigation GPS.

Geomechanical properties of the mobilized material were characterized using geotechnical testing. Three unaltered
135 geotechnical soil samples were extracted for a direct shear test (Figure 1). The samples were extracted from a depth of 40 cm (41.1843ºS , 72.4652ºW) to avoid integrating possible organic material in each sample. Because the soil corresponds to a granular soil, we used a split cube (Table 1). The sampling probe was removed from unsaturated media without water table presence. The sample water content was determined by drying at a constant temperature of 60° C (ASTM, 2019). The geotechnical shear test was carried out deforming a specimen at a constant controlled stress rate throughout the period of
140 deformation based on ASTM D3080 / D3080M-11 standard (ASTM D3080, 2020). The estimated values of the cohesion and internal friction angle were integrated into a database to be used during the back analysis phase.

Table 1 Properties obtained by direct shear test. Geotechnical results incorporated into the r.avaflow model as constraints.

Physical properties per test sample			
Physical properties	Test sample 1	Test sample 2	Test sample 3
Water content (%)	3.31	3.30	3.27
Natural density (kg/m^3)	1620	1560	1630
Density (kg/m^3)	1570	1510	1580
Density after consolidation (kg/m^3)	1670	1600	1640
Lateral displacement rate used (mm/min)	0.50	0.50	0.50
Lateral displacement achieved (%)	10.00	10.00	10.00
Maximum shear stress (N/m^2)	71589	50014	33343
Normal stress (N/m^2)	78453	39227	19613

3.2 Debris flow modelling

Representing debris flows is currently a challenge due to the possible changes of phase, which may occur during the process
145 from generation to stabilization. Therefore, the r.avaflow model was used to evaluate the fall of blocks on saturated/unsaturated zones and their subsequent evolution as non-Newtonian flow (Mergili et al., 2017; Mergili et al., 2018b). Measurements of soil water content into the fall of blocks are not available. Therefore, various water content scenarios were carried out.

3.2.1 Back-analysis

The r.avaflow model was applied by back analysis, taking as constraints the cohesion data and the angle of internal friction
150 obtained from the undisturbed soil samples collected in the field (Figure 1). The back-analysis considered a final height of 1.5

m in route CH255, according to reports of National Geological and Mining Survey (SERNAGEOMIN in Spanish). Moreover, volumes of liberation zone were integrated from the evidence collected in the field. The model used a two-phase parametrization based on Pudasaini (2012). First, the solid phase corresponds to the lava and auto-breccia fall; meanwhile, the second phase is associated with the debris flow generation under saturated/non-saturated water conditions. During the solid

155 phased, a mohr ‑coulomb plasticity approach allowed it to be estimated for the stress. The fluid stress was modeled as a solid ‑ volume ‑fraction ‑gradient ‑enhanced non ‑Newtonian viscous stress (Pudasaini, 2012; Mergili et al., 2017). Let $u_s = (u_s, v_s, w_s)$, $u_f = (u_f, v_f, w_f)$ and α_f, $\alpha_f = (1 - \alpha_s)$ denote the velocities, and volume fractions for the solid and the fluid constituents, denoted by the suffix s and f, respectively, where η_f correspond to the fluid viscosity with isotropic stress distribution and $A(\alpha_f)$ is called the mobility of the fluid at the interface. The phase-averaged viscous-fluid stresses are modelled using non-Newtonian

160 fluid rheology:

$$\tau_f = \eta_f \left[\nabla \underline{u_f} + \left(\nabla \underline{u_f} \right)^t \right] - \eta_f \frac{A(\alpha_f)}{\alpha_f} \left[(\nabla \alpha_s) \left(\underline{u_f} - \underline{u_s} \right) + (u_f - u_s)(\nabla \alpha_s) \right]$$

(1)

The back analysis used a generalized interfacial momentum transfer that included viscous drag, buoyancy, and virtual mass. Non-Newtonian viscous stress was based on Pudasaini and Mergili (2019), separating the solid- and fine-solid- volume fraction

165 gradients, enhancing the apparent viscous stress estimation in the fluid phase. Parameters not measured in the field were established from similar works and data from the area of Villa Santa Lucía (Somos-Valenzuela et al., 2020; Table 2). We selected model parameters to the range proposed by Pudasaini (2012) for the simulation of debris flows. We compared height flow with the calibration point (route CH-255), discarding unreasonable simulations.

Surface features such as slope are important input data for debris-flow modelling [Qin et al., 2013]. DEM errors introduce

170 uncertainty in terrain representation leading to a poor estimation of the numerical solutions. Given the uncertainty of the (DEM before the 2017 Petrohué event, two DEMs were used as references to assess the sensitivity of changes in elevation. The SRTM and ASTER-GDEM models were used separately, with a spatial resolution of 30 meters due to data availability limitations. The possible release zones or areas of origin of these debris flows were established from the geomorphological evidence found in the field. The results of the back analysis were compared with photographs provided by the Chilean Geology and Mining

175 Survey (SERNAGEOMIN) based on "El Solitario" (~ 41.180ºS, 72.462ºW) to assess the performance of the models with different initial water contents.

Table 2 Model parameters used in r.avaflow.

Symbol	Parameter	Value	units
ρ_s	Solid material density	2800	kg/m^3
ρ_f	Fluid material density	1000	kg/m^3
ϕ	Internal friction angle *	32.4	Degree

δ	Basal friction angle	6	Degree
C	Virtual mass	0.5	-
U_T	Terminal velocity	1	m/s
P	Parameter for combination of solid- and fluid-like contributions to drag resistance	0.5	-
Re_p	Particle Reynolds number	1	-
J	Exponent for drag	1	-
N_R	Quasi-Reynolds number	4,5	-
N_{RA}	Mobility number	3	-
x	Viscous shearing coefficient for fluid	0	-
ξ	Solid concentration distribution with depth	0	-
C_{AD}	Ambient drag coefficient	0,02	-
C_E	Entrainment coefficient	-6.69	kg^{-1}
C_{FF}	Fluid friction coefficient	0.001	

3.2.2 Sensitivity analysis

180 A systematic study has been carried out to represent the debris flow. Mergili et al. (2018a) established that parameters with high sensitivity correspond to the basal friction angle, fluid friction coefficient, and environmental drag coefficient. We used reference values previously considered in the zone (Somos-Valenzuela et al., 2020). Moreover, geotechnical laboratory tests allowed to represent the friction angle and cohesion values adequately. Sources of uncertainty were attributed to surface representation and initial water content in the head of block fall. A wide range of initial water content was considered,

185 constrained by the geomorphological evidence at the site, to calibrate the model to observations in the field. Since the initial proportion of water when the hyper-concentrated flow was generated is unknown, we assumed a water content in the initial volume between 40% up to 70%, considering the high porosity of the material involved. Hence, we calibrate the flow runout taking control points of the height of the flow measured on the main road minutes after the event. The percentual error was calculated using the height simulated with the measured height in "El Solitario pass". A percentual difference was used between

190 the simulated value and the measured height divided by the measured height. We also assessed the quality of the simulations using possible release volumes based on field evidence.

3.2.3   Projections

Finally, possible scenarios evaluating the impact of new debris flows in the area were analyzed. Therein, we defined new unstable release zones identified visually in the field. We identify areas with intense rain erosion, hanging blocks, or fractured rocks. This enabled us to estimate the potential volume transported, and thus to understand the impact of different debris flows generated in zones that were very close together, but with release at different altitudes.

4   Results

The conditions that generate debris flows were evaluated in an active volcanic zone, with reference to the 2017 Petrohué event. Information collected in the field was assessed and compared with numerical modelling using back analysis with r.avaflow.

4.1   Field evidence

The debris flow in the distal zone is characterized by poorly sorted volcanic material. The deposited material is supported by a medium-coarse sand matrix (2 mm) along with > 1-meter diameter blocks. The mode of the clasts in the sandy matrix varies between 3 to 10 cm, being consistent with previous results (Garrido et al., 2017). Moreover, lateral erosion after the debris flow shows a highly energetic process. Geotechnical measurements showed low unit weight (Table 2) supporting that the thickness of the flow is moderated. These favours a faster movement, increasing lateral erosion according to field results [Shu et al., 2018]. The lahar deposits show granulometric differences, with strong graduation from the fracture zone (proximal zone) to the final deposition zone (distal zone). From 400 masl, volcanic deposits alternate with autobrecciated lava flows (Figure 3). The walls are up to 20 meters high with high stratification and different grain size. A pronounced difference in competence was observed between the volcanic deposits and the autobrecciated lava flows, which facilitates differential erosion and planes of weakness (Figure 4).

Field evidence showed that debris flows are generated by the fracture of basaltic lava over volcanic deposits in the high altitude zone of the study area. Rockfalls occurring above 1500 m.a.s.l. were identified (Figure 1 and Figure 4). This zone presents numerous scarps with pronounced slopes overhanging fluvial drain channels (Figure 3). The remains of the debris flow identified in the field are associated with transported blocks of basaltic lava and primary lahar deposits.

The incision is favoured by the presence of very thick lahar deposits (Figure 3), which facilitate the removal and contribution of material to the main channel. A sequence of lahar deposits was observed, overlain by lava flows in blocks up to 1.5 m thick. These occur in regular sequences, leaving alternate levels of erosion and hanging blocks, facilitating the collapse of the lava levels, and generating rockfalls. The material is characterized by lava with base autobrecciation, no more than 1 m thick (Figure 3). The autobrecciated zone is also heavily weathered (Figure 4); as a result, it can be easily removed, exposing the centre of the lava flow. The lava flow forms a hanging block that can easily fracture and break off. There is evidence of broken-

off blocks associated with the central part of the lava flow, due to the instability of the base autobrecciation, with dimensions of up to 2 m. The blocks fracture continuously in the lava runs perpendicular to the slope of the main channel where these debris flows occur. This breaking off of material due to weathering contributes to the main channel, generating powerful debris flows as evidenced by the deposits further down the slope, as a consequence of the continuous rockfalls. The intermediate zone

225 has narrow drainage channels and an increase in the incision to a depth of around 15 m (Figure 3).

Figure 3 Fifteen-metre high scarp showing the stratigraphy of the volcano at this point, composed of alternating volcanic and lava deposits.

Figure 4 Set of scarps at approximately 1500 masl; the base breccia of the lava flows is heavily eroded.
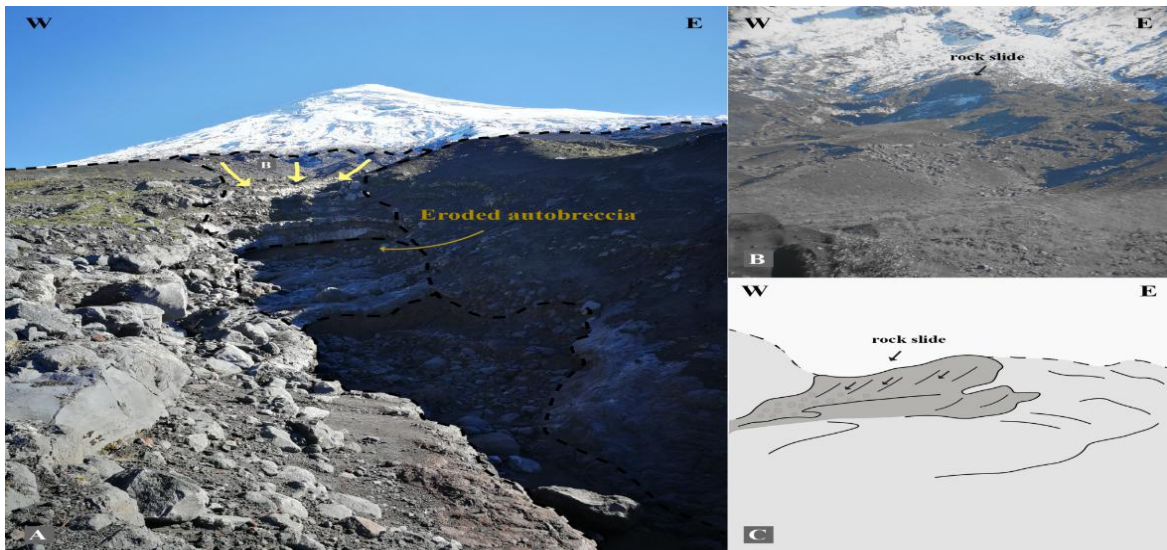
230

4.2   Debris flow modelling

To understand the scope of the runout generated in the release zones of material recognized in the field, the flow was modelled in r.avaflow. Different initial water content into the simulations and DEMs differences allowed understood the uncertainty of the main initial input. The results of the back analysis, restricted by geotechnical soil data, showed that the model that presented the smallest mean error was the simulation using DEM SRTM and 70% water content (error 5%). The results show that in both simulations, the flow covers a large part of Route CH-255, to a 1.59 meters depth with DEM SRTM and 1.58 meters depth with DEM ASTER (Figure 5). Our results indicate that DEM ASTER presented a larger underestimation of the height of -25% with a water content of 65%. With a water content of 40%, DEM ASTER produces an overestimation of 63% against the value measured. These results suggest that the initial quantity of water during the collapse has a large influence on the area affected.

The area affected by the debris flow was estimated at between 7.5 million m^2 and 7.8 million m^2 by DEM ASTER, and between 8.3 million m^2 and 8.6 million m^2 by DEM SRTM (Figure 5a). Simulations using DEM SRTM produced a variation of the flow to the south, increasing the impact in Route CH-255. These results had differences with the simulations using DEM ASTER, which showed the flow towards the north (Figure 6). The maximum height was calculated at between 5.55 and 6.74 meters by DEM ASTER, and between 6.33 and 7.69 meters by DEM SRTM. A progressive increase in the maximum height as the percentage of water in the release zone increased was noted in the simulations. DEM SRTM presented greater heights than DEM ASTER in all the simulations. The major debris flow height is reached when the initial volume has 70% of the water in both DEMs. Finally, all the simulations reached populated zones, regardless of the DEM used. The maximum height

250 with DEM SRTM is 1.87 meters with a water content of 40% of the initial water content, while with DEM ASTER, it is 2.13 meters with a water content of 60%. The greatest heights are concentrated with a water content of 50%-60% of the total material released.

Figure 5 Backanalysis results.
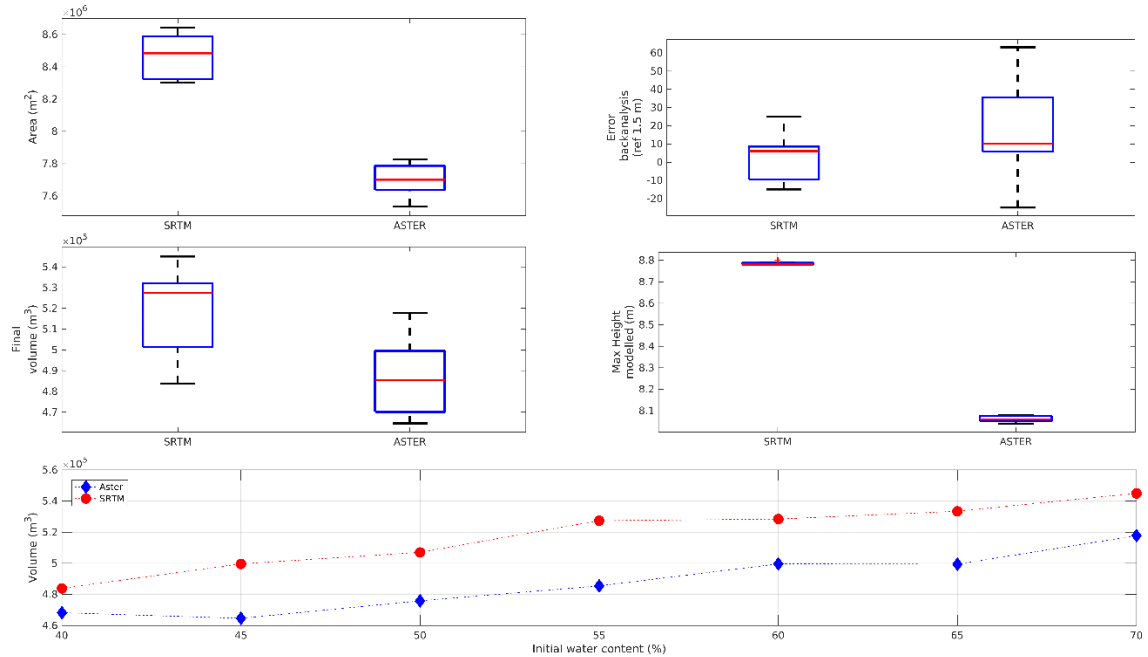
255 Figure 6 Simulation in El Solitario sector, taking the release zone from the results obtained in the field. Left: Model with 60% water content in DEM ASTER. Right: Model with 60% water content in DEM STRM.

Debris flow height (m)

0.28 - 0.74	2.90 - 3.38
0.75 - 1.28	3.39 - 3.99
1.29 - 1.82	4.00 - 4.95
1.83 - 2.35	4.96 - 6.55
2.36 - 2.89	6.56 - 9.08

Symbology

- - - - - Scarp
::::::: Boundaries debris flow
● Error back-analysis
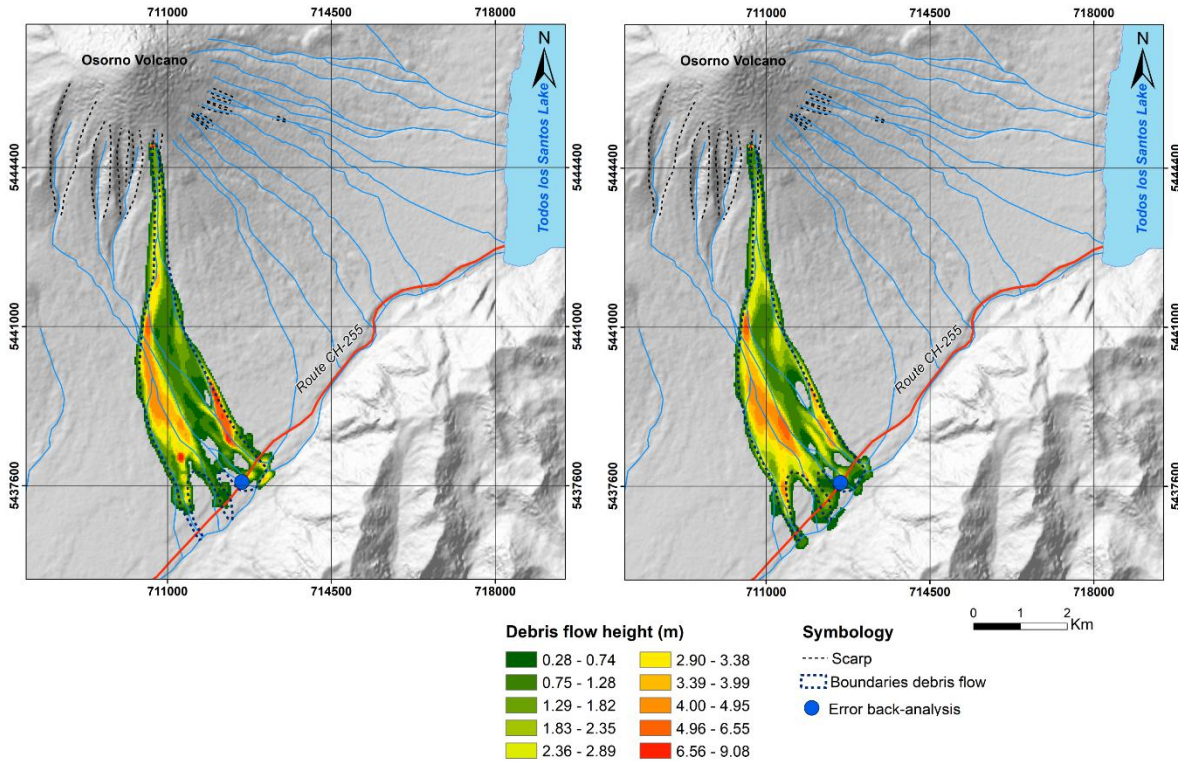
In addition to the zone identified as the source of the Petrohué event of 2017, three zones with unstable autobrecciated lava were catalogued as possible debris flow generation zones (Figure 1 and Figure 4). The information collected in the field showed

260 that the gullies in these zones are severely weakened, so debris flows produced by rockfalls can be expected imminently. Additional release zones to those in r.avaflow were estimated with calibration based on the parameters of the back analysis model. Our results indicate that the area potentially affected by the debris flow varies between 3.1 million m^2 and 3.8 million m^2 using DEM ASTER, and between 1.3 million m^2 and 4.4 million m^2 using DEM SRTM (Figure 7). DEM SRTM produces the largest area affected with 60% water content in the initial volume released and DEM ASTER with 70%.

265 According to the back analysis, a rockfall with 50% water content is capable of transporting a potential volume of 138,628 m^3; the potential with 70% water is 148,830 m^3. According to DEM SRTM, the potential volume with 50% water content is 32,039 m^3, increasing to 177,399 m^3 with 70% water. In this case, the greatest volume is generated when the proportion of water is equal to 70% of the volume initially released, and the highest value is given by DEM SRTM simulation. The lowest value is obtained with a water content of 50%, using DEM SRTM. Finally, the maximum height for DEM SRTM is 0.76 meters, when

270 the water content is 70% of the volume released. In this simulation in DEM ASTER, the debris flow would not reach Route CH-255 (Figure 7). Our results indicate that the flow released from zone 2 with 60% water content will reach a minimum

height of 1.82 meters in populated zones. Likewise, there are cases in which the debris flow will not necessarily reach the populated zones, suggesting that events of this type are not always recorded.

Figure 7 Impact of different debris flows.
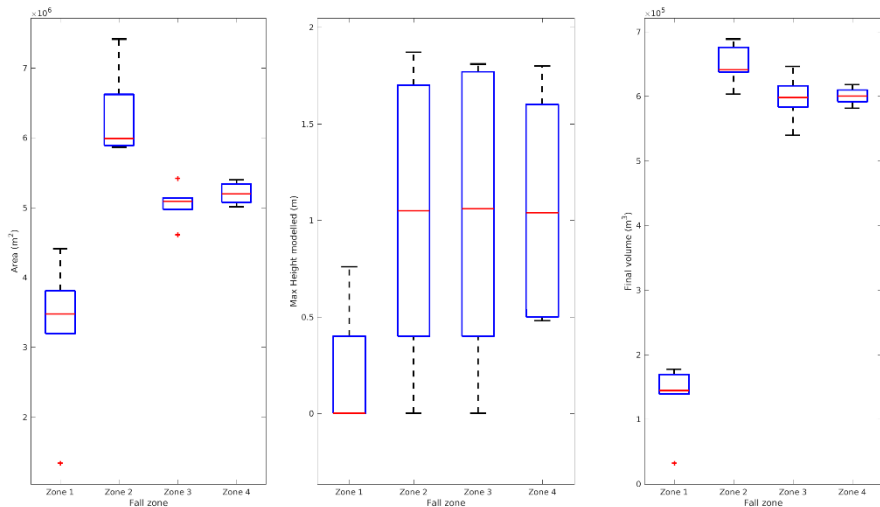
Finally, our results indicate the existence of events that will not generate debris flows even if there is a fall of lava blocks in the channel. This can be seen in zone 1, identified by the evidence collected in the field as an area in which debris flows are generated. On the other hand, a hypothetical scenario of a debris flow generated in zone 2 could lead to debris flows with larger volumes than those observed in previous events (Figure 7). Likewise, it can generate greater flow heights than values recorded to date, leading to more catastrophic events in populated zones. This risk has not been considered to date and needs to be assessed with care.

5   Analysis and Discussion

5.1   Field evidence

The geomorphology of the Osorno volcano is characterized by the alternation of basaltic lava flows overlain by large volcanic deposits (Figure 3). The fractures identified in the lava flows were probably generated by gravitational effects. Water can then enter the rock/soil fractures, making them more likely to break off and transporting the material in debris flow form. Conditions are therefore favorable for chain processes culminating in debris flows when the soil is saturated by high altitude rainfall. Erosion of the deposits exposes the lava flows; material breaks away and is transported by gravity and/or swept down by the

force of the water. Furthermore, the autobrecciation of the lava flows increases the instability of the rock faces in the release
290   zones due to the high porosity of the material (Vezzoli et al., 2017; Schaefer et al., 2018).

The evidence collected in the field showed a heterogeneous distribution of lava and slopes close to the debris flow release zones. In this way, the magnitude and force of the landslides processes may be affected by the spatial distribution of volcanic products, principally lava flows. The results show that above 600 masl, there are many exposed lava layers at the base of the principal fluvial channels. A bedrock channel could increase the velocity of the flow in comparison to an alluvial-type channel.
295   This characteristic suggests that the base could act as a sliding surface for the material (Dufresne et al., 2019), which is very common in stratovolcanoes in Southern Andes. It could be a smooth surface with lower friction, especially under rainy conditions. This could have a critical influence on the velocity and acceleration of the flow from the higher reaches of the edifice. Lavigne & Suwa (2004), Sheridan et al. (2005), and Aaron & Hungr (2016) suggest that the dynamic of debris flows depends upon the friction of the base surface. Having said this, the distribution of the lava and its autobrecciation play an
300   important role in the generation of landslides, rockfalls, and debris flows in the study zone (Figure 8).

Figure 8 A. Distal zone in an alluvial deposit in the El Solitario sector. B. Alluvial deposit with thick of 1.2 m; the base level presents flow structures with fluvial erosion.
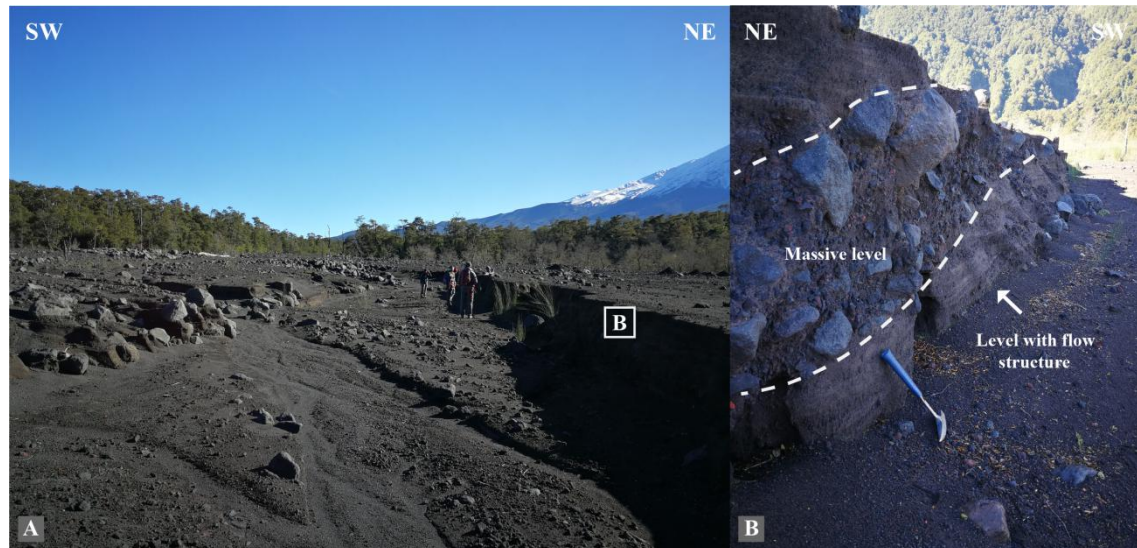
305   5.2   Debris flow modelling

Our results represented the dynamic of the 2017 Petrohué debris flow with variable errors in the back analysis. Our models were consistent with results obtained in the field, showing a strong influence on the initial water content. The simulations present high sensitivity to the water content previous to the generation of the event – all the simulations in which the water content in the release zone was higher than 45% reached populated zones. The calibration parameters played an important role

310 in the sensitivity of the numerical model. In the present study, the drag coefficient was established at 0.020, based on Zwinger et al. (2003) and Oyarzún (2019); this value was adopted due to the degree of optimization in the back analysis. A larger or smaller coefficient could produce large deviations in the final height and direction of the flow (Mergili et al., 2018a). The angle of internal friction was determined by a geotechnical study. However, the heterogeneity of the zone could produce substantial changes in φ, so this value must be assessed with great care in future cases. This introduces great uncertainty into

315 the models due to the existence of an imminent bias in the results. It is clear from our results that the use of a DEM introduces a bias in the modelling, which may be directly linked with the methodology by which each product is created and the date of acquisition (e.g., Kääb et al., 2005; Bühler et al. 2011). It must be remembered that processes may occur, which produce changes in the relief that the DEM is unable to capture due to low spatial resolution (Figure 8A and Figure 8B). Alganci et al. (2018) report that SRTM has better vertical accuracy (8.5 m) vs ASTER GDEM (16 m). Vertical uncertainty provides wrong

320 flow routing values, overestimating the final height in some cases. Therefore, DEM product could introduce an additional uncertainty which must be analyzed carefully during calibration and interpretation. Nonetheless, back analysis allows us to estimate variations in the volumes transported and their extreme values, with variation within the same order of magnitude (Figure 6).

The results show that the scope of the debris flow is proportional to the initial water content. Thus the water content available

325 during the collapse of material at the 1500 m contour allows events to occur, which will reach populated zones. Our results show that debris flows are dangerous if the collapse happens with saturation over 50%. We propose that the presence of water in the release zone is explained by local hydrometeorological conditions, i.e., rainfall at high altitude; this is consistent with similar events at Villa Santa Lucía (Garrido et al., 2018; Somos-Valenzuela et al., 2020).

The differences between the initial and final volumes suggest the incorporation of material into the debris flow due to the

330 erosion, which causes movement of the flow (Figure 9). This is supported by evidence in the field, which showed that movable material is available between the distal and proximal zones (Figure 8B). Retreating scarps were observed, which continuously add material to the drainage networks, and this material is available when debris flows occur. Our field results indicate that the largest volume of the material comes from volcanic deposits (Figure 8A).

Figure 9 Conceptual model of chain processes in Osorno Volcano.
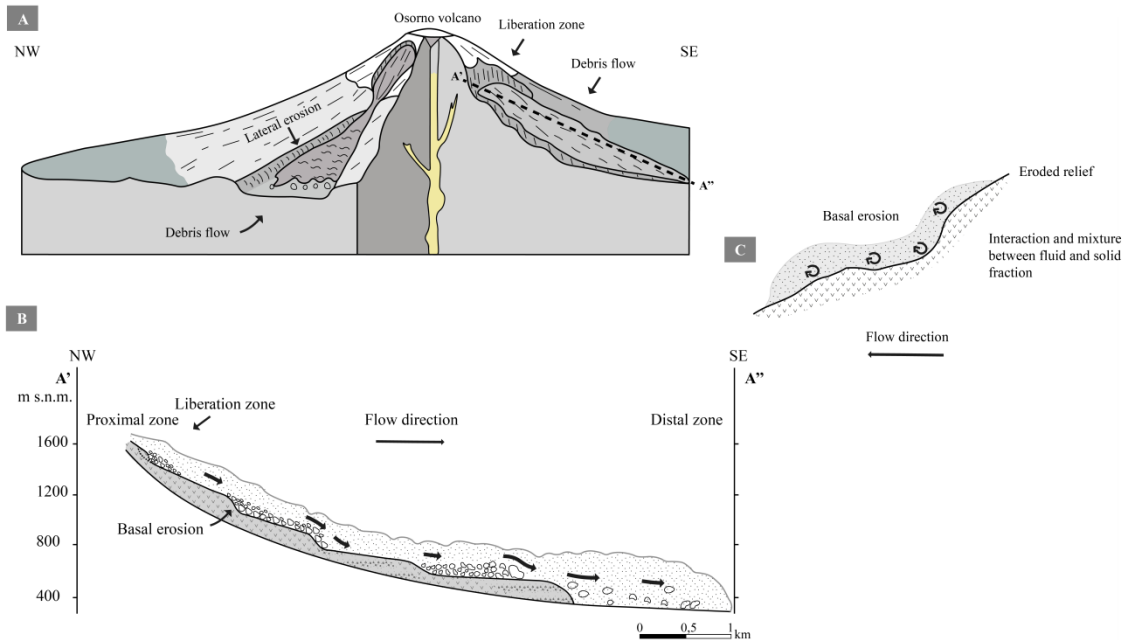
335

Finally, water-rich mass flows are distinguished by material type, water content, the presence of excess pore pressure, or liquefaction at the source (Calhoun & Clague, 2018). We controlled possible sources of uncertainty such as lithology and topography through a terrain analysis that allowed reducing degrees of freedom. Therefore, the initial water content becomes

340 an important independent variable due to the unknown value during the main event. The gap of soil moisture stations close to the liberation zone does not allow to constrain the numerical solution with precise detail. Our results show debris-flow generation over 50% of initial water content. The final volume variation of the debris flow varies between 4.8 to 5.6 x 10^5 m^3. The DEM SRTM showed small errors in comparison to ASTER, so, we establish that the volume estimated from SRTM is more suitable for our case. Moreover, SRTM showed more area affected in comparison to ASTER by the debris flow. We

345 propose that the use of an SRTM scenario correspond to an accurate solution considering lesser error and conservative solutions for future debris flow events. However, we do not establish preliminary conditions for soil liquefaction. To the future, this issue will need to be addressed carefully to improve our understanding of the flow-type landslide in volcanic environments.

5.3   Future implications

Our projections indicate that the danger to populated areas is strongly dependent on the release zone of debris flows (Figure

350 7). This suggests that debris flows may repeatedly occur, which are not observed because they are remote from populated areas, increasing the structural destabilization of the volcano in the long term. The release volumes calculated in the present

study were defined according to the current stability conditions observed in the field; however, more intense precipitations could lead to more significant rainfall erosion of transportable material (Figure 8B), favouring increasingly violent debris flows. Such scenarios require the appropriate authorities to propose road design projects as a matter of urgency to evacuate the

355 flows quickly and efficiently. This will improve the mitigation efforts to prevent the population from becoming cut off from the rest of the country. Finally, the geomorphology of the Osorno volcano is not unique in the Southern Andes. For example, Villarrica and Llaima volcanoes show similar conditions to Osorno. We thus have firm grounds for assuming that unexpected debris flows could occur elsewhere in southern Chile, with the difference that these volcanoes are in more densely populated zones, exposing the population to even more danger.

360 6   Conclusion

The 2017 Petrohué event was studied by back analysis to understand the impact of debris flows occurring on active volcanoes in the Southern Andes. We used comprehensive in-situ data to constrain a numerical model for understanding the debris flow event. We evaluate the liberation zone for Osorno Volcano, showing that debris flows occur due to the collapse of autobrecciated lava flows above 1500 m.a.s.l. for the first time (Figure 9A). Geomorphological in-situ data determined that

365 the debris flow was a combination of factors such as fluvial erosion and the composition of the volcano, both of which together led to a loss of stability (Figure 9B). The succession of volcanic deposits and autobbreciated lava flows generate conditions for the development of debris flows. Geomorphological evidence has shown that block falls and slips occurring mainly above 1500 m a.s.l. becoming into debris flows, increasing the volume transported to the base of the volcano (Figure 9C). Simulations in r.avaflow showed that the debris-flow volume varies between 464,564 m3 and 544,903 m3, depending on the

370 amount of water available. Moreover, debris flow from only 45% of water content may reach the populated areas. Hence, the water available is critical in the rockfall zone in the first steps of the debris flow. Debris flows projections indicate that the final volume generated could vary between 32,039 and 688,142 m3 depending on the initial water content and generation zone in the volcano. Small debris-flow volumes projected suggest that it could be generated continuously without reach populated areas. Moreover, constant erosive processes could cause larger rockfalls and slips, causing more catastrophic events in the

375 future. Therefore, the Osorno volcano needs to be taken into account as a hot spot for debris-flow monitoring. Finally, our results report for the first time a case of debris flow on a stratovolcano in the southern Andes from its generation, using data collection in situ and modelling with sensitivity analysis using a two-phase model. Our conclusion is to urge the scientific community to focus efforts on generating scenarios for debris flows in the stratovolcanoes of the southern Andes. The population density around Osorno volcano is low but receives a high number of tourists every year However, the areas of

380 stratovolcanoes like Villarrica and Calbuco contain higher population densities, and these volcanoes must not be ignored in future territorial plans. The present study shows evidence that the debris flows identified are recurrent events, even though they do not always reach populated areas. Our results show that this threat is inherent to volcanic activity, so any future risk

analysis must consider debris flows. This will allow better risk management in nearby population centres and a safer coexistence with the volcanic structures of the southern Andes.

Author contributions

IF and BM contributed to the conceptualization and methodology of the research and performed the formal analysis, visualization, and validation. IF and MS was involved in the funding and supervision of the paper. IF and PM contributed with the supervision, review, and editing of the paper. RM, IR and NC provided input in terms of methodology and the review and editing of the paper.

Competing interests

The authors declare that they have no conflict of interest.

Financial support

This was made possible thanks to the "Agencia Nacional de Investigación y Desarrollo (ANID)" of the Chilean government, grant number PII180008 and the "Fondecyt Iniciación" program (grant no. 11180500). We acknowledge Dirección de Investigación of the University of La Frontera for their English editing support.

References

Aaron J and Hungr O. 2016. Dynamic analysis of an extraordinarily mobile rock avalanche in the Northwest Territories, Canada. Can Geotech J, 53:899–908. doi:10.1139/cgj-2015-0371.

Aguilar G, Carretier S, Regard V et al. 2014. Grain size-dependent 10Be concentrations in alluvial stream sediment of the Huasco Valley, a semi-arid Andes region. Quaternary Geochronology, 19:163–172. doi:10.1016/j.quageo.2013.01.011.

Alimohammadlou Y, Najafi A and Yalcin A. 2013. Landslide process and impacts: A proposed classification method. CATENA, 104:219–232. doi:10.1016/j.catena.2012.11.013.

Alganci U, Besol B & Sertel E. 2018. Accuracy Assessment of Different Digital Surface Models. IJGI, 7:114. doi:10.3390/ijgi7030114.

ASTM. 2017. D2487-17e1, Standard Practice for Classification of Soils for Engineering Purposes (Unified Soil Classification System), ASTM International, West Conshohocken, PA, 2017, www.astm.org. doi: 10.1520/D2487-17E01

ASTM. 2019. D2216-19, Standard Test Methods for Laboratory Determination of Water (Moisture) Content of Soil and Rock by Mass, ASTM International, West Conshohocken, PA, 2019. doi. 10.1520/D2216-19

410 ASTM D3080 / D3080M-11 (2020b), Standard Test Method for Direct Shear Test of Soils Under Consolidated Drained Conditions (Withdrawn 2020), ASTM International, West Conshohocken, PA, 2011, www.astm.org. doi 10.1520/d3080_d3080m-11

Bühler Y, Christen M, Kowalski J et al. 2011. Sensitivity of snow avalanche simulations to digital elevation model quality and resolution. Ann Glaciol, 52:72–80. doi:10.3189/172756411797252121.

415 Bueechi E, Klimeš J, Frey H et al. 2018. Regional-scale landslide susceptibility modelling in the Cordillera Blanca, Peru—a comparison of different approaches. Landslides, 16:395–407. doi:10.1007/s10346-018-1090-1.

Calhoun NC & Clague JJ. 2018. Distinguishing between debris flows and hyperconcentrated flows: an example from the eastern Swiss Alps. Earth Surf Process Landforms, 43:1280–1294. doi:10.1002/esp.4313.

Cembrano J & Lara L. 2009. The link between volcanism and tectonics in the southern volcanic zone of the Chilean Andes:
420 A review. Tectonophysics, 471:96–113. doi:10.1016/j.tecto.2009.02.038.

Dufresne A, Wolken GJ, Hibert C et al. 2019. The 2016 Lamplugh rock avalanche, Alaska: deposit structures and emplacement dynamics. Landslides, 16:2301–2319. doi:10.1007/s10346-019-01225-4.

Evans SG, Bishop NF, Fidel Smoll L et al. 2009. A re-examination of the mechanism and human impact of catastrophic mass flows originating on Nevado Huascarán, Cordillera Blanca, Peru in 1962 and 1970. Engineering Geology, 108:96–118.
425 doi:10.1016/j.enggeo.2009.06.020.

Fustos I, Abarca-del-Rio R, Moreno-Yaeger P et al. 2020. Rainfall-Induced Landslides forecast using local precipitation and global climate indexes. Nat Hazards, 102:115–131. doi:10.1007/s11069-020-03913-0.

García-Delgado H, Machuca S & Medina E. 2019. Dynamic and geomorphic characterizations of the Mocoa debris flow (March 31, 2017, Putumayo Department, southern Colombia). Landslides, 16:597–609. doi:10.1007/s10346-018-01121-3.

430 Garrido, N. (2015). Deslizamientos y flujos de detritos en Petrohué, Sierra Santo Domingo, naciente río Petrohué ladera sur. 02.06.2015. Servicio Nacional de Geología y Minería, Informe Técnico, 11 p.

Garrido, N., Mella, M., Sepúlveda, V., Duhart, P., Moreno, H. (2017). Efectos geológicos de los flujos de detritos ruta CH-225 entre Ensenada y Petrohué, 08 de enero 2017, región de Los Lagos (INF-X-05.2017) [informe inédito]. Puerto Varas: Sernageomin, 2017. 12.

435 Garrido, N., Sepúlveda, V., Duhart, P. (2018). Catastro de remociones en masa de la Provincia de Llanquihue, Región de Los Lagos (INF-Los Lagos-10.2018) [informe inédito]. Puerto Varas, Sernageomin, 2018.

INE (2018). ENCUESTA MENSUAL DE ALOJAMIENTO TURÍSTICO, AÑO 2017. Technical report. Document available at https://www.ine.cl/docs/default-source/actividad-del-turismo/publicaciones-y-anuarios/informe-anual/informe-anual-emat-2017.pdf (last access 12/06/2020)

440 Jakob, M., Hungr, O., & Jakob, D. M.. 2005. Debris-flow Hazards and Related Phenomena, Springer Berlin Heidelberg. p.

Johnson JB & Palma JL. 2015. Lahar infrasound associated with Volcán Villarrica's 3 March 2015 eruption. Geophys Res Lett, 42:6324–6331. doi:10.1002/2015gl065024.

Kääb A, Huggel C, Fischer L et al. 2005. Remote sensing of glacier- and permafrost-related hazards in high mountains: an overview. Nat Hazards Earth Syst Sci, 5:527–554. doi:10.5194/nhess-5-527-2005.

445 Korup, O., Seidemann, J., & Mohr, C. H. (2019). Increased landslide activity on forested hillslopes following two recent volcanic eruptions in Chile. Nature Geoscience, 12(4), 284-289.

Lavigne F & Suwa H. 2004. Contrasts between debris flows, hyperconcentrated flows and stream flows at a channel of Mount Semeru, East Java, Indonesia. Geomorphology, 61:41–58. doi:10.1016/j.geomorph.2003.11.005.

Major JJ, Bertin D, Pierson TC et al. 2016. Extraordinary sediment delivery and rapid geomorphic response following the 2008-2009 eruption of Chaitén Volcano, Chile. Water Resour Res, 52:5075–5094. doi:10.1002/2015wr018250.

450

Martha TR, Kerle N, Jetten V et al. 2010. Characterising spectral, spatial and morphometric properties of landslides for semi-automatic detection using object-oriented methods. Geomorphology, 116:24–36. doi:10.1016/j.geomorph.2009.10.004.

Mergili M, Fischer J-T, Krenn J et al. 2017. r.avaflow v1, an advanced open-source computational framework for the propagation and interaction of two-phase mass flows. Geosci Model Dev, 10:553–569. doi:10.5194/gmd-10-553-2017.

455 Mergili M, Frank B, Fischer J-T et al. 2018a. Computational experiments on the 1962 and 1970 landslide events at Huascarán (Peru) with r.avaflow: Lessons learned for predictive mass flow simulations. Geomorphology, 322:15–28. doi:10.1016/j.geomorph.2018.08.032.

Mergili M, Emmer A, Juřicová A et al. 2018b. How well can we simulate complex hydro-geomorphic process chains? The 2012 multi-lake outburst flood in the Santa Cruz Valley (Cordillera Blanca, Perú). Earth Surf Process Landforms, 43:1373–1389. doi:10.1002/esp.4318.

460

Moreno, H., Lara, L.E., Orozco, G. 2010. Geología del volcán Osorno, Región de Los Lagos. Servicio Nacional de Geología y Minería, Carta Geológica de Chile, Serie Geología Básica 126: p., 1 mapa escala 1:50.000, Santiago.

Moreno, H., Varela, J., López-E,L., Munizaga, F., Lahsen, A. 1985. Geología y riesgo volcánico del volcán Osorno y centros eruptivos menores, Universidad de Chile, Departamento de Geología y Geofisica, 212 p. Sangiago

465 Moreno, T., & Gibbons, W. (Eds.). 2007. The geology of Chile. Geological Society of London.

NARANJO JL, SIGURDSSON H, CAREY SN et al. 1986. Eruption of the Nevado del Ruiz Volcano, Colombia, On 13 November 1985: Tephra Fall and Lahars. Science, 233:961–963. doi:10.1126/science.233.4767.961.

Oyarzún, J. (2019). Análisis de los factores gatillantes al flujo hiperconcentrado en Villa Santa Lucía y determinación de las condicionantes de un proceso futuro. Trabajo de Proyecto de Titulación para optar al Título de Ingeniero Civil. Universidad de La Frontera, Facultad de Ingeniería y Ciencias.

470

Pierson TC. 1995. Flow characteristics of large eruption-triggered debris flows at snow-clad volcanoes: constraints for debris-flow models. Journal of Volcanology and Geothermal Research, 66:283–294. doi:10.1016/0377-0273(94)00070-w.

Pierson TC, Major JJ, Amigo Á et al. 2013. Acute sedimentation response to rainfall following the explosive phase of the 2008–2009 eruption of Chaitén volcano, Chile. Bull Volcanol, 75. doi:10.1007/s00445-013-0723-4.

475 Pudasaini SP. 2012. A general two-phase debris flow model. J Geophys Res, 117:n/a-n/a. doi:10.1029/2011jf002186.

Pudasaini SP and Mergili M. 2019. A Multi‑Phase Mass Flow Model. J Geophys Res Earth Surf, 124:2920–2942. doi:10.1029/2019jf005204.

Qin C-Z, Bao L-L, Zhu A-X et al. 2013. Uncertainty due to DEM error in landslide susceptibility mapping. International Journal of Geographical Information Science, 27:1364–1380. doi:10.1080/13658816.2013.770515.

480 Rodríguez I, Páez J, van Wyk de Vries MS et al. 2020. Dynamics and physical parameters of the Lastarria debris avalanche, Central Andes. Journal of Volcanology and Geothermal Research, 402:106990. doi:10.1016/j.jvolgeores.2020.106990.

Schaefer LN, Kennedy BM, Villeneuve MC et al. 2018. Stability assessment of the Crater Lake/Te Wai-ā-moe overflow channel at Mt. Ruapehu (New Zealand), and implications for volcanic lake break-out triggers. Journal of Volcanology and Geothermal Research, 358:31–44. doi:10.1016/j.jvolgeores.2018.06.011.

485 Schuster RL, NietoThomas AS, D. O'Rourke T et al. 1996. Mass wasting triggered by the 5 March 1987 ecuador earthquakes. Engineering Geology, 42:1–23. doi:10.1016/0013-7952(95)00024-0.

Sepúlveda SA, Moreiras SM, Lara M et al. 2014. Debris flows in the Andean ranges of central Chile and Argentina triggered by 2013 summer storms: characteristics and consequences. Landslides, 12:115–133. doi:10.1007/s10346-014-0539-0.

Sheridan MF, Stinton AJ, Patra A et al. 2005. Evaluating Titan2D mass-flow model using the 1963 Little Tahoma Peak
490 avalanches, Mount Rainier, Washington. Journal of Volcanology and Geothermal Research, 139:89–102. doi:10.1016/j.jvolgeores.2004.06.011.

Shu H, Ma J, Yu H et al. 2018. Effect of Density and Total Weight on Flow Depth, Velocity, and Stresses in Loess Debris Flows. Water, 10:1784. doi:10.3390/w10121784.

Sosio R, Crosta GB & Hungr O. 2011. Numerical modeling of debris avalanche propagation from collapse of volcanic edifices.
495 Landslides, 9:315–334. doi:10.1007/s10346-011-0302-8.

Somos-Valenzuela MA, Oyarzún-Ulloa JE, Fustos-Toribio IJ et al. 2020. The mudflow disaster at Villa Santa Lucía in Chilean Patagonia: understandings and insights derived from numerical simulation and postevent field surveys. Nat Hazards Earth Syst Sci, 20:2319–2333. doi:10.5194/nhess-20-2319-2020.

Stern CR. 2007. Holocene tephrochronology record of large explosive eruptions in the southernmost Patagonian Andes. Bull
500 Volcanol, 70:435–454. doi:10.1007/s00445-007-0148-z.

Tacconi Stefanelli C, Vilímek V, Emmer A et al. 2017. Morphological analysis and features of the landslide dams in the Cordillera Blanca, Peru. Landslides, 15:507–521. doi:10.1007/s10346-017-0888-6.

Thouret J-C, Antoine S, Magill C et al. 2020. Lahars and debris flows: Characteristics and impacts. Earth-Science Reviews, 201:103003. doi:10.1016/j.earscirev.2019.103003.

505 Vezzoli L, Apuani T, Corazzato C et al. 2017. Geological and geotechnical characterization of the debris avalanche and pyroclastic deposits of Cotopaxi Volcano (Ecuador). A contribute to instability-related hazard studies. Journal of Volcanology and Geothermal Research, 332:51–70. doi:10.1016/j.jvolgeores.2017.01.004.

Wieczorek, G.F., Larsen, M.C., Eaton, L.S., et al. 2000. Catastrophic landslides and flooding in coastal Venezuela, December 16, 1999 (abstr.). In Program with abstracts, 2000 Annual Meeting, Assoc. of Engrg. Geologists, San Jose, California, 19-26

510 Sept., AEG News, Vol. 43, No. 4, p. 120.

Zwinger T, Kluwick A & Sampl P. 2003. Numerical Simulation of Dry-Snow Avalanche Flow over Natural Terrain. In: Dynamic Response of Granular and Porous Materials under Large and Catastrophic Deformations. Springer Berlin Heidelberg, p. 161–194.

515